



Effect of Cu ion substitution on structural and dielectric properties of Ni–Zn ferrites

Guang-sheng LUO^{1,2,3}, Wei-ping ZHOU^{1,2,4}, Jian-de LI³, Gui-wen JIANG³, Shao-long TANG^{1,2}, You-wei DU^{1,2}

1. National Laboratory of Solid State Microstructures, Nanjing University, Nanjing 210093, China;

2. Department of Physics, Nanjing University, Nanjing 210093, China;

3. Academy of Space Technology, Nanchang University, Nanchang 330031, China;

4. Department of Applied Physics, School of Science,
Nanjing University of Science and Technology, Nanjing 210094, China

Received 17 July 2015; accepted 10 October 2015

Abstract: A series of Cu-substituted $\text{Ni}_{0.5-x}\text{Cu}_x\text{Zn}_{0.5}\text{Fe}_2\text{O}_4$ ($x=0.12, 0.16, 0.20, 0.24$ and 0.28) spinel ferrites were prepared by conventional ceramic method to investigate the effects of Cu compositional variation on the structure and dielectric properties. XRD patterns demonstrate that all the samples are crystallized in single-phase cubic spinel structure and the lattice constant increases with increasing Cu content. White grains observed by SEM are Cu-rich phase. The dielectric constant versus frequency curve displays a normal dielectric behavior of spinel ferrites. While the frequency dependence of dielectric loss tangent is found to be abnormal, exhibiting a peak at certain frequency for all Cu-substituted Ni–Zn ferrites. A maximum of the resistivity is observed at $x=0.2$ due to the decrease of hopping electrons between Fe^{2+} and Fe^{3+} in per unit volume, which is in contrast with the Cu content dependence of dielectric constant and dielectric loss.

Key words: ferrite; Cu ion substitution; dielectric constant; dielectric dispersion; dielectric loss; resistivity

1 Introduction

Spinel ferrite materials are well-known important function materials and frequently used in fabrication of multilayer chip inductor, which can be applied as surface mounted device in microelectronic devices, such as transformer, sensor, digital diary and floppy disk drive [1–6]. The substitutions of spinel ferrite materials with proper ions prepared by different methods have become more and more important both in fundamental and application point of view [5–7]. Particularly, the mixed Ni–Zn ferrite is the most versatile ferrite from the viewpoint of its extensive use in high-frequency applications and electronic industry, due to its high value of magnetization, high permeability and low power loss at high frequencies, high Curie temperature, high resistivity, high quality factor and low dielectric loss [3,8,9]. Recent interest in the study of spinel ferrites is in terms of their synthesis and sintering at low temperatures as well as on nano-sized ferrite materials

for various applications [8,10,11]. The requirement for making multilayer chip inductor is that the insulating ferrite layer is co-fired with silver internal electrode at low temperature (900 °C, generally is 870 °C) to prevent reaction with the electrode materials, and the low temperature sintered ferrite powder should be suitable to taper-casting process. It is reported that the addition of CuO in Ni–Zn ferrite would promote grain growth, improve the sinterability and lower the sintering temperature of ferrites, resulting in the increase in grain size, which would benefit for making multilayer chip inductor [6,10,12]. In this regard, compared with Ni–Zn ferrite, the Ni–Cu–Zn ferrite which possesses lower sintering temperature and excellent electromagnetic properties is a kind of magnetic materials with great potential applications in multilayer chip inductor. It is known that the properties of spinel ferrite are strongly influenced by their composition and microstructure which can be modified by doping with proper ions [4,5]. Therefore, it is of particular interest to investigate the effect of Cu content on the dielectric properties of Ni–Zn

ferrite. In this work, a series of $\text{Ni}_{0.5-x}\text{Cu}_x\text{Zn}_{0.5}\text{Fe}_2\text{O}_4$ ferrites ($x=0.12, 0.16, 0.20, 0.24, 0.28$) were prepared through the conventional ceramic method, and their microstructure and dielectric properties with the variation of Cu doping ratio were focused.

2 Experimental

Fe_2O_3 , NiO, ZnO and CuO of analytic purity were used as raw materials to prepare the $\text{Ni}_{0.5-x}\text{Cu}_x\text{Zn}_{0.5}\text{Fe}_2\text{O}_4$ ferrites by conventional ceramic method. After first ball-milling of 3 h, these mixtures were pre-sintered at 850 °C for 3 h. Then a second ball-milling was performed for 6 h. Moderate amount of PVA (10%) was added as binder. After that, these mixtures were pressed into pellets with diameter of 14 mm and thickness of 4 mm under a pressure of 100 MPa, followed by sintering at 1000 °C for 4 h with heating rate of 5 °C/min and then furnace cooling to room temperature. The phase purity and structure were characterized by X-ray powder diffraction (XRD) with Cu K_α ($\lambda=1.5405$ Å) radiation (BRUKER, D8 Focus) at room temperature. The scan range 2θ was 20°–80°, the scan step is 0.02°, the integral time was 1 s, the tube voltage was 40 kV and the tube current was 40 mA. The microstructures were characterized by HITACHI S-3000N scanning electron microscope. For the measurement of dielectric properties, all the samples were cut into plates with parallel wide faces, and sintered silver was used as electrodes on both wide sides. The resistivity of all the samples was measured by two-probe method. The dielectric constant and dielectric loss were measured by Agilent 4284A LCR meter in the frequency range of 20 Hz–1 MHz. Dielectric constant can be calculated by the formula [13,14]:

$$\varepsilon' = \frac{C_p t}{\varepsilon_0 A} \quad (1)$$

where ε' is the dielectric constant, ε_0 is the permittivity of vacuum (8.854×10^{-2} pF/cm), C_p is the capacitance of sample, t is the thickness of the sample and A is the cross sectional area of the sample. While the dielectric loss ($\tan \delta$) can be calculated by the following equation:

$$\tan \delta = \frac{1}{Q} \quad (2)$$

where Q is the quality factor of the sample.

3 Results and discussion

Figure 1 shows the XRD patterns of $\text{Ni}_{0.5-x}\text{Cu}_x\text{Zn}_{0.5}\text{Fe}_2\text{O}_4$ ($x=0.12, 0.16, 0.20, 0.24, 0.28$) samples. As we can see, all the five samples are crystallized in spinel structure with strong diffraction peaks, demonstrating

that all the samples are well crystallized at sintering temperature of 1000 °C and the grains grow uniformly. The average grain size estimated by Scherrer formula is 53–60 nm. As shown in Table 1, the lattice parameters of these Cu-substituted ferrites increase with increasing Cu content. The reason can be explained by the larger ionic radius of Cu^{2+} (0.73 Å) compared with Ni^{2+} (0.69 Å) [15]. When parts of Ni^{2+} are substituted by Cu^{2+} , the unit cell is expanded, leading to a larger lattice constant.

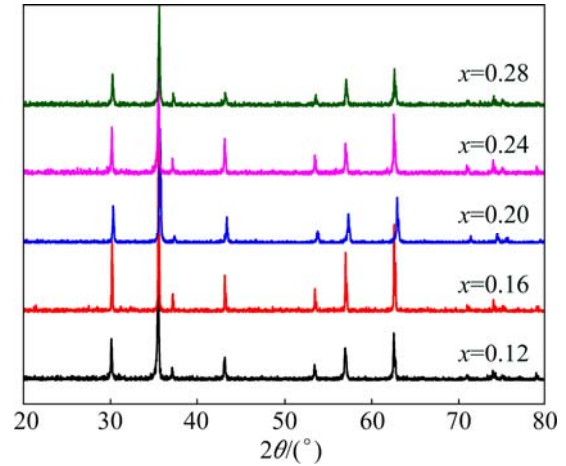


Fig. 1 XRD patterns of $\text{Ni}_{0.5-x}\text{Cu}_x\text{Zn}_{0.5}\text{Fe}_2\text{O}_4$ samples

Table 1 Lattice parameter, grain size and density for $\text{Ni}_{0.5-x}\text{Cu}_x\text{Zn}_{0.5}\text{Fe}_2\text{O}_4$ ferrites

x	Lattice constant/Å	Grain size/nm	Density/($\text{g}\cdot\text{cm}^{-3}$)
0.12	8.32	53.2	5.21
0.16	8.35	53.8	5.18
0.20	8.37	53.6	5.15
0.24	8.41	56.3	5.17
0.28	8.44	59.5	5.19

Figure 2 displays the SEM images of these Cu-substituted Ni–Zn ferrites. As we can see, the grain size gradually increases with increasing Cu content. The average grain sizes of samples with Cu contents $x=0.12, 0.16, 0.20, 0.24$ and 0.28 are 3.0, 3.6, 4.3, 5.1 and 6.7 μm , respectively. The growth of grains with increasing Cu content can be explained by the liquid phase formation in the sintering process, where the existence of liquid phase would increase the atomic mobility. With increasing the content of Cu in the sample, the amount of liquid phase in the sintering process increases, resulting in the grain growing larger. In the samples of $x=0.12, 0.16, 0.20$ and 0.24 , white particles can be observed between grain boundaries in the SEM images. HSU et al [16] have confirmed that the phase segregated at grain boundary is the Cu-rich phase, which have never been observed in Ni–Zn ferrites prepared by any other methods. As shown

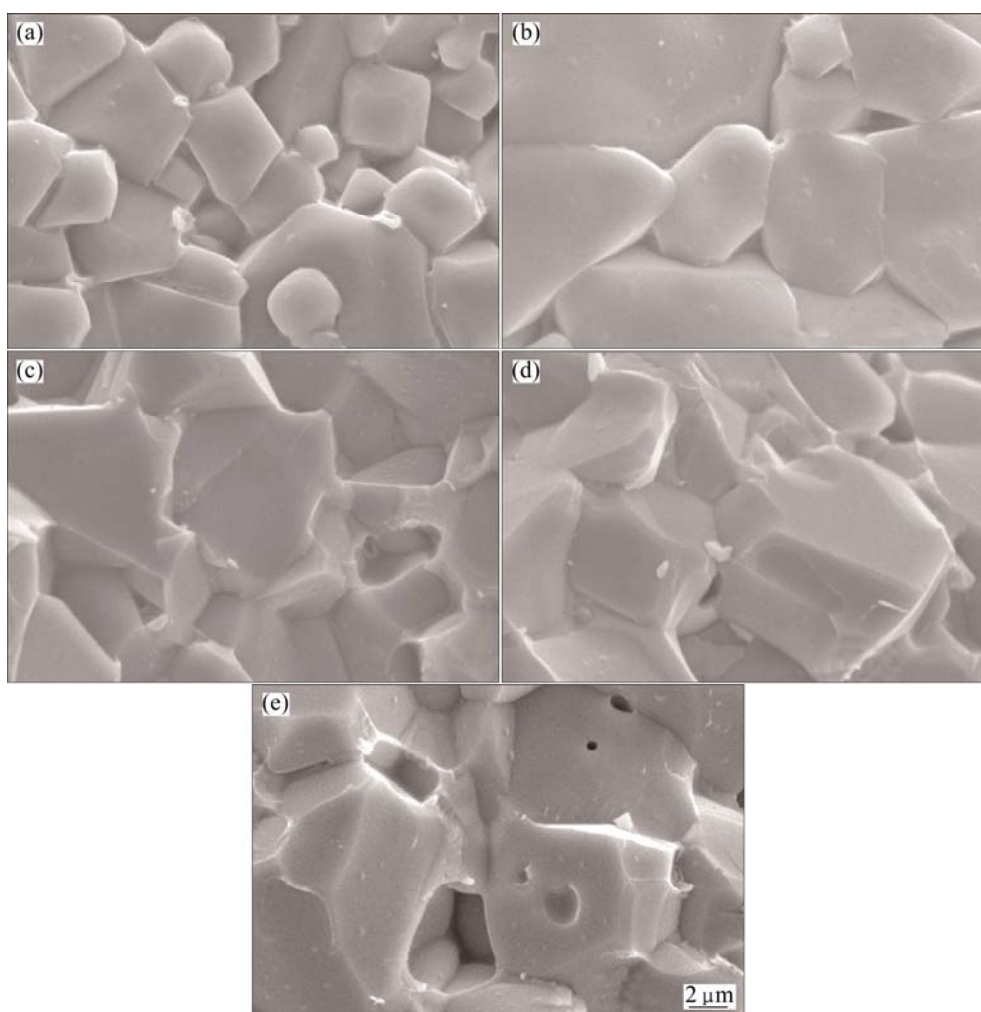


Fig. 2 SEM images of $\text{Ni}_{0.5-x}\text{Cu}_x\text{Zn}_{0.5}\text{Fe}_2\text{O}_4$ ferrites: (a) $x=0.12$; (b) $x=0.16$; (c) $x=0.20$; (d) $x=0.24$; (e) $x=0.28$

in the SEM image of sample with $x=0.28$, grains excessively grow due to the existence of liquid phase, leading to the occurrence of bubbles and the densification of grains.

Then, we have characterized the dielectric properties of Ni–Cu–Zn ferrites in the frequency range of 20 Hz–1 MHz at room temperature. As can be seen in Fig. 3, the dielectric constants of these samples with different Cu content decrease with increasing frequency. The dielectric dispersion observed at low frequency is large, but it does not change obviously with the frequency of electric field in high frequency, displaying a normal dielectric phenomenon. This kind of dielectric phenomenon can be ascribed to the dielectric polarization in ferrites, and the dielectric process is similar with the conduction mechanism which can be explained by the Verwey–de-Boer hopping mechanism [17]. VERWEY and HAAYMAN [17] have considered that the reason for the electric conduction in ferrites is the electron hopping between ions of the same element with different valence states, and these ions are occupied

on the same lattice position. The gather of Fe^{2+} is a kind of typical character in ferrites, which depends on several factors such as sintering temperature, sintering time and crystal structure. The formation of Fe^{2+} gives rise to electron hopping between Fe^{2+} and Fe^{3+} , i.e., the $\text{Fe}^{2+}/\text{Fe}^{3+}$ electric dipoles are formed along the direction of external electric field, consequently electric polarization is generated in the ferrites [18]. The number of electrons hopping between Fe^{2+} and Fe^{3+} is dependent on the number of $\text{Fe}^{2+}/\text{Fe}^{3+}$ dipoles on B site. With the increase of frequency, the dielectric constant continuously decreases and finally approaches to a constant value. This behavior can be ascribed to the frequency of electrons hopping between Fe^{2+} and Fe^{3+} dipoles unable to keep pace with the frequency of external alternating electric field when exceeding a certain frequency. A similar dielectric behavior is observed in Mg–Cu–Zn ferrites [19].

As shown in Fig. 3, the dielectric constant in low frequency can reach up to 10^4 – 10^5 . Such large dielectric constant in low frequency can be explained by

Maxwell–Wagner interfacial polarization theory [20], and is in consistent with Koops theory [21]. Inhomogeneous dielectric structures in ferrites are supposed to be composed of two layers; one is ferrite grains with good conductivity, and the other is grain boundaries with inferior conductivity, wherein grains are surrounded by grain boundaries. It is reported that grain boundaries with inferior conductivity are very active in low frequency, while grains with good conductivity play a role in high frequency, which explains the reason why large dielectric constant is observed in low frequency and low dielectric constant is observed in high frequency in ferrites [22]. According to Koops model [21], grains and boundaries can be regarded as one system in polycrystalline ferrites. In this system, large grains (ε_1, ρ_1) with low resistivity are separated by thin boundaries (ε_2, ρ_2) with high resistivity. KOOPS [21] has assumed that $x=d_2/d_1 \leq 1$, $\rho_1 \leq \rho_2$, and $\varepsilon_1 \approx \varepsilon_2$, and the dielectric constant of sample can be expressed as

$$\varepsilon' = \frac{\varepsilon_1}{x} - \frac{\varepsilon_2}{x} \quad (3)$$

where x is the thickness of grain boundary, ε_1 and ε_2 are dielectric constants of grain and boundary, while ρ_1 and ρ_2 are resistivities of grain and boundary, respectively. Therefore, the dielectric constant in low frequency is determined by grain boundary. The thinner the boundary is, the larger the dielectric constant is.

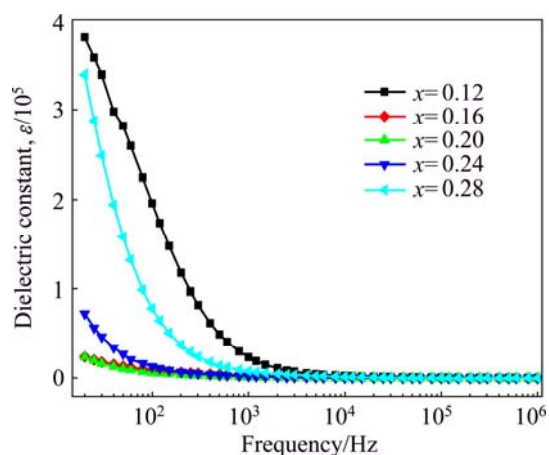


Fig. 3 Dielectric constant (ε) as function of frequency for $\text{Ni}_{0.5-x}\text{Cu}_x\text{Zn}_{0.5}\text{Fe}_2\text{O}_4$ ferrites

As shown in Fig. 4, the variation of dielectric constant is decreased first and then increased with the increase of Cu content, exhibiting a minimum at $x=0.2$. The dielectric constant in the frequency range of 10 kHz–1 MHz is lower than that of Ni–Zn ferrites prepared by the same method. For Ni–Cu–Zn ferrites, the value of dielectric constant is 10^2 – 10^3 compared with that of 10^3 – 10^4 for Ni–Zn ferrite in the frequency range of 10 kHz–1 MHz [21]. The relatively low melting point

of CuO can reduce the sintering temperature of Ni–Zn ferrite because the melting CuO acts as liquid phase in the sintering process, suppressing the formation of Fe^{2+} and polarization in ferrites. As a result, the number of electrons hopping between Fe^{2+} and Fe^{3+} decreases and therefore the dielectric constant decreases.

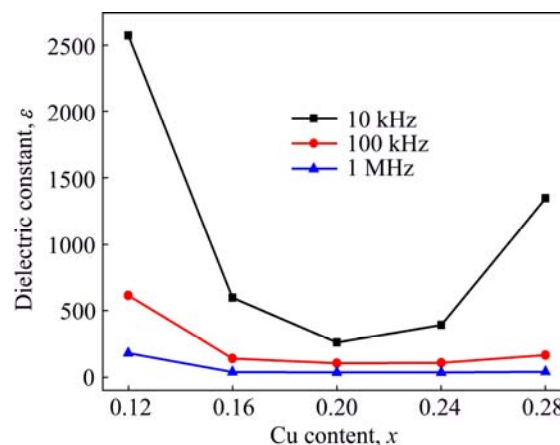


Fig. 4 Compositional variation of dielectric constant for $\text{Ni}_{0.5-x}\text{Cu}_x\text{Zn}_{0.5}\text{Fe}_2\text{O}_4$ ferrites

The density also has a great impact on the dielectric properties of polycrystalline ferrites. As we can see from Table 1, the density decreases first and then increases as a function of substituted Cu content, which reaches a maximum at $x=0.12$. All the samples are denser than Ni–Zn ferrites because the added CuO acts as liquid phase in the sintering process which could increase the lattice diffusion. From Fig. 2, we can see that the grains are uniform at $x=0.12$ with the maximum density. However, at $x=0.16, 0.20, 0.24$ and 0.28 , micropores are observed in grains, which can account for the decrease of density. But the structure becomes denser at $x=0.24$ and 0.28 , resulting in a small rise of density. The denser the sample is, the more number of $\text{Fe}^{2+}/\text{Fe}^{3+}$ dipoles are in per unit volume. Therefore, there are more hopping electrons between Fe^{2+} and Fe^{3+} dipoles, thus the dielectric constant is enhanced. As shown in Fig. 4, the dielectric constant exhibits a minimum at $x=0.2$, which is in accordance with the variation of density. MUKESH et al [23] have obtained maximum sintered density when the substituted Cu content is $x=0.1$ in Ni–Zn ferrite, with a similar result of minimum density at $x=0.2$.

Figure 5 present the frequency dependence of dielectric loss. As shown in the figure, the dielectric loss curves for all the samples are not in accordance with the dielectric constant curves and loss peaks are observed for all the samples in a certain frequency, exhibiting an abnormal dielectric behavior. This kind of dielectric behavior has been reported in Ni–Mg ferrites [24]. The peak position in dielectrics can be determined by the following equation:

$$\omega\tau=1 \quad (4)$$

where $\omega=2\pi f_{\max}$, τ is the relaxation time which is related to the electron hopping time p through formula $\tau=1/2p$ or $f_{\max}\propto p$. When the time of electron hopping between Fe^{2+} and Fe^{3+} is comparable with the frequency of external alternating electric field, a maximum of dielectric loss can be observed, which is termed as ferromagnetic resonance [25]. The maximum values observed in samples with $x=0.12, 0.16, 0.24$ and 0.28 are much more than that in sample with $x=0.20$, indicating that the amount of hopping electrons which conform to this requirement in unit time at a certain frequency is increasing. This can be ascribed to the increasing amount of Fe^{2+} gathered on B site, leading to a reduction of resistivity, which is in accordance with Fig. 7. As shown in Fig. 6, the dielectric losses of samples with different Cu contents at high frequency are much lower than those in low frequency, suggesting the potential application in high frequency of Cu-substituted Ni–Zn ferrites.

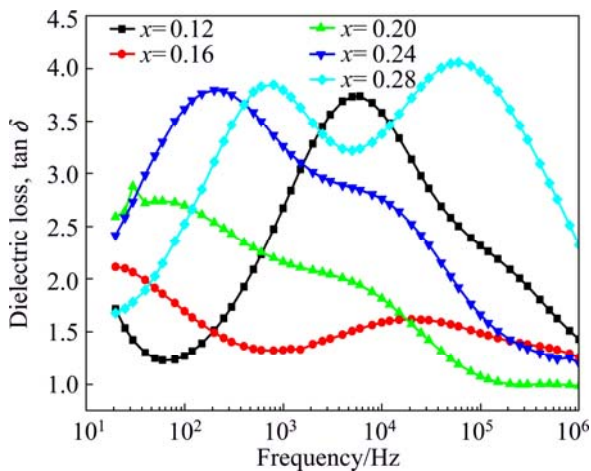


Fig. 5 Dielectric loss as function of frequency for $\text{Ni}_{0.5-x}\text{Cu}_x\text{Zn}_{0.5}\text{Fe}_2\text{O}_4$ ferrites

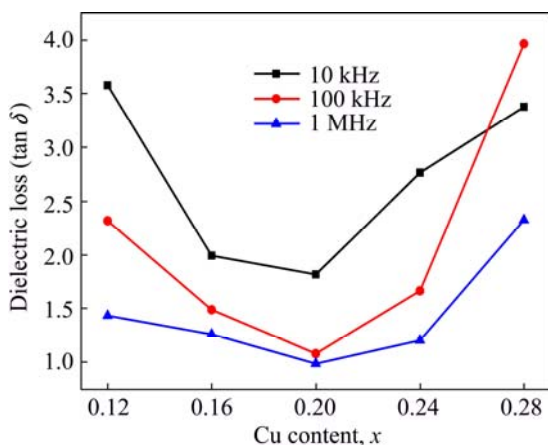


Fig. 6 Compositional variation of dielectric loss of $\text{Ni}_{0.5-x}\text{Cu}_x\text{Zn}_{0.5}\text{Fe}_2\text{O}_4$ ferrites

As can be seen from Fig. 4 and Fig. 7, the variation of resistivity as a function of Cu content is in contrast with that of dielectric constant and dielectric loss. A large resistivity is corresponding to a small dielectric constant while a small resistivity is corresponding to a large dielectric constant. The resistivity is also determined by the amount of electrons hopping between Fe^{2+} and Fe^{3+} . The more the number of electrons hopping between Fe^{2+} and Fe^{3+} is, the smaller the resistivity value is. Therefore, the larger the dielectric constant is, the more the number of Fe^{2+} on B site and the number of electrons hopping between $\text{Fe}^{2+}/\text{Fe}^{3+}$ are, thus, the conductivity of ferrite becomes better, resulting in a reduction of resistivity. As we can see from Fig. 7, the resistivity increases first and then decreases as a function of Cu content with a maximum at $x=0.2$, which is corresponding to a minimum of dielectric constant and dielectric loss. The resistivity of $\text{Ni}_{0.5-x}\text{Cu}_x\text{Zn}_{0.5}\text{Fe}_2\text{O}_4$ ($x=0.12, 0.16, 0.20, 0.24, 0.28$) is in the range of 10^4 – $10^6 \Omega\cdot\text{cm}$, which is larger than that of Ni–Zn ferrites reported by ZHENG et al [26] with the same preparation method. The reason can be ascribed to that the addition of Cu ions would reduce the sintering temperature and result in a reduction of Fe^{2+} , which suppresses the opportunities of electron hopping between Fe^{2+} and Fe^{3+} , leading to the increase of resistivity.

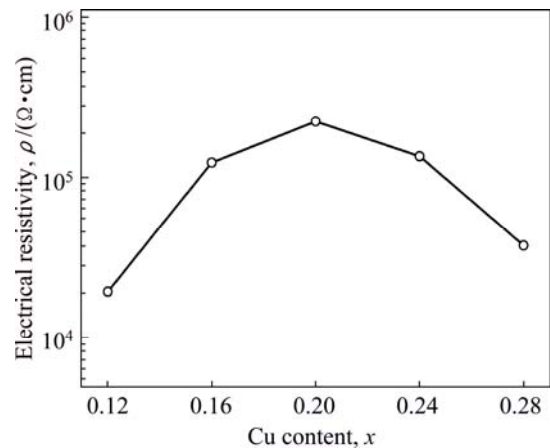


Fig. 7 Compositional variation of electric resistivity of $\text{Ni}_{0.5-x}\text{Cu}_x\text{Zn}_{0.5}\text{Fe}_2\text{O}_4$ ferrites

4 Conclusions

1) The substitution of Cu ions in Ni–Zn spinel ferrites can effectively influence their structures and microstructures properties. XRD patterns demonstrate that all the samples are crystallized in single-phase cubic spinel structure and the lattice constant increases with increasing Cu content due to the larger ionic radius of Cu^{2+} compared with that of Ni^{2+} . This confirms that the white particles segregated at grain boundaries observed in SEM images are the Cu-rich phase.

2) Furthermore, the variation of Cu content in Ni–Zn spinel ferrites can effectively modify their dielectric and electric properties. The dielectric constant decreases with increasing frequency, and the dielectric dispersion observed in low frequency is larger compared with that in high frequency. An abnormal dielectric behavior with dielectric loss peak is observed in the dielectric loss vs frequency curve. The resistivity of Ni–Zn ferrites increases first and then decreases with the variation of Cu content, exhibiting a maximum at $x=0.2$ because the number of electron hopping between Fe^{2+} and Fe^{3+} in per unit volume is reduced for the lowest density of this doping ratio. While the dielectric constant and dielectric loss as a function of Cu doping ratio display a minimum at $x=0.2$ due to the decrease of hopping electrons between Fe^{2+} and Fe^{3+} in per unit volume.

References

- [1] MATSUO Y, INAGAKI M, TOMOZAWA T, NAKAO F. High performance NiZn ferrite [J]. *IEEE Transactions on Magnetism*, 2001, 37(4): 2359–2361.
- [2] SHINDE T J, GADKARI A B, VASAMBEKAR P N. Magnetic properties and cation distribution study of nanocrystalline Ni–Zn ferrites [J]. *Journal of Magnetism and Magnetic Materials*, 2013, 333(0): 152–155.
- [3] NASIR S, SALEEMI A S, FATIMA-TUZ-ZAHRA, ANIS-UR-REHMAN M. Enhancement in dielectric and magnetic properties of Ni–Zn ferrites prepared by sol–gel method [J]. *Journal of Alloys and Compounds*, 2013, 572: 170–174.
- [4] GABAL M A, AL-ANGARI Y M, AL-AGEL F A. Cr-substituted Ni–Zn ferrites via oxalate decomposition: Structural, electrical and magnetic properties [J]. *Journal of Magnetism and Magnetic Material*, 2015, 391: 108–115.
- [5] KUMBHAR S S, MAHADIK M A, MOHITE V S, RAJPURE K Y, KIM J H, MOHOLKAR A V, BHOSALE C H. Structural, dielectric and magnetic properties of Ni substituted zinc ferrite [J]. *Journal of Magnetism and Magnetic Materials*, 2014, 363: 114–120.
- [6] HAN Q J, JI D H, TANG G D, LI Z Z, HOU X, QI W H, LIU S R, BIAN R R. Estimating the cation distributions in the spinel ferrites $\text{Cu}_{0.5-x}\text{Ni}_{0.5}\text{Zn}_x\text{Fe}_2\text{O}_4$ ($0.0 \leq x \leq 0.5$) [J]. *Journal of Magnetism and Magnetic Materials*, 2012, 324(12): 1975–1981.
- [7] BATOO K M. Structural and electrical properties of Cu doped NiFe_2O_4 nanoparticles prepared through modified citrate gel method [J]. *Journal of Physics and Chemistry of Solids*, 2011, 72(12): 1400–1407.
- [8] KAMBALE R C, ADHATE N R, CHOUGULE B K, KOLEKAR Y D. Magnetic and dielectric properties of mixed spinel Ni–Zn ferrites synthesized by citrate-nitrate combustion method [J]. *Journal of Alloys and Compounds*, 2010, 491(1–2): 372–377.
- [9] SU Hua, ZHANG Huai-wu, TANG Xiao-li, JING Yu-lan. Microstructure and magnetic properties of Ni–Zn ferrites doped with MnO_2 [J]. *Transactions of Nonferrous Metals Society of China*, 2011, 21(1): 109–113.
- [10] SU Hua, TANG Xiao-li, ZHANG Huai-wu, JING Yu-lan, ZHONG Zhi-yong. Low-temperature-fired NiCuZn ferrites with BBSZ glass [J]. *Journal of Magnetism and Magnetic Materials*, 2011, 323(5): 592–595.
- [11] BATOO K M, ABD EL-SADEK M S. Electrical and magnetic transport properties of Ni–Cu–Mg ferrite nanoparticles prepared by sol–gel method [J]. *Journal of Alloys and Compounds*, 2013, 566: 112–119.
- [12] BATOO K M, ANSARI M S. Low temperature-fired Ni–Cu–Zn ferrite nanoparticles through auto-combustion method for multilayer chip inductor applications [J]. *Nanoscale Research Letters*, 2012, 7(1): 1–14.
- [13] SHAIKH P A, KAMBALE R C, RAO A V, KOLEKAR Y D. Studies on structural and electrical properties of $\text{Co}_{1-x}\text{Ni}_x\text{Fe}_{1.9}\text{Mn}_{0.1}\text{O}_4$ ferrite [J]. *Journal of Alloys and Compound*, 2009, 482(1–2): 276–282.
- [14] KAMBALE R C, SHAIKH P A, BHOSALE C H, RAJPURE K Y, KOLEKAR Y D. Dielectric properties and complex impedance spectroscopy studies of mixed Ni–Co ferrites [J]. *Smart Material and Structures*, 2009, 18(8): 085014.
- [15] JADHAV P A, DEVAN R S, KOLEKAR Y D, CHOUGULE B K. Structural, electrical and magnetic characterizations of Ni–Cu–Zn ferrite synthesized by citrate precursor method [J]. *Journal of Physics and Chemistry of Solids*, 2009, 70(2): 396–400.
- [16] HSU W C, CHEN S C, KUO P C, LIEA C T, TSAIA W S. Preparation of NiCuZn ferrite nanoparticles from chemical co-precipitation method and the magnetic properties after sintering [J]. *Materials Science and Engineering B*, 2004, 111(2–3): 142–149.
- [17] VERWEY E J W, HAAYMAN W P. Electronic conductivity and transition point of magnetite (“ Fe_3O_4 ”) [J]. *Physica*, 1941, 8: 979–987.
- [18] KOLEKAR C B, KAMBLE P N, KULKARNI S G, VAINGANKAR A S. Effect of Gd^{3+} substitution on dielectric behaviour of copper-cadmium ferrites [J]. *Journal of Materials Science*, 1995, 30(22): 5784–5788.
- [19] HAQUEA M M, HUQA M, HAKIMB M A. Densification, magnetic and dielectric behavior of Cu-substituted Mg–Zn ferrites [J]. *Materials Chemistry and Physics*, 2008, 112(21): 580–586.
- [20] MAXWELL J C. A treatise on electricity and magnetism [M]. Oxford, London: Clarendon Press, 1982.
- [21] KOOPS C G. On the dispersion of resistivity and dielectric constant of some semiconductors at audio frequencies [J]. *Physical Review*, 1951, 83: 121–124.
- [22] IWAUCHI K. Dielectric properties of fine particles of Fe_3O_4 and some ferrites [J]. *Japanese Journal of Applied Physics*, 1971, 10: 1520–1528.
- [23] MUKESH C D, VERMA A, SUBHASH C K, DUBEA D C, THAKURB O P, PRAKASHB C. Structural, dielectric and magnetic properties of NiCuZn ferrite grown by citrate precursor method [J]. *Materials Science and Engineering B*, 2006, 133: 42–48.
- [24] VARSHNEY D, VERMA K. Substitutional effect on structural and dielectric properties of $\text{Ni}_{1-x}\text{A}_x\text{Fe}_2\text{O}_4$ (A = Mg, Zn) mixed spinel ferrites [J]. *Materials Chemistry and Physics*, 2013, 140: 412–418.
- [25] RABKIN L I, NOVIKOVA Z I. Ferrites [M]. *Izv Acad: Nauk USSR Minsk*, 1960: 146.
- [26] ZHENG H, WENG W, HAN G, DU P. Colossal permittivity and variable-range-hopping conduction of polarons in $\text{Ni}_{0.5}\text{Zn}_{0.5}\text{Fe}_2\text{O}_4$ ceramic [J]. *The Journal of Physical Chemistry C*, 2013, 117(25): 12966–12972.

Cu 离子掺杂对 Ni-Zn 铁氧体结构和介电性能的影响

罗广圣^{1,2,3}, 周卫平^{1,2,4}, 李建德³, 姜贵文³, 唐少龙^{1,2}, 都有为^{1,2}

1. 南京大学 固体微结构国家实验室, 南京 210093;
2. 南京大学 物理学院, 南京 210093;
3. 南昌大学 空间科学与技术研究院, 南昌 330031;
4. 南京理工大学 理学院 应用物理系, 南京 210094

摘要: 通过传统的陶瓷制备工艺制备了一系列 Cu 掺杂的 $\text{Ni}_{0.5-x}\text{Cu}_x\text{Zn}_{0.5}\text{Fe}_2\text{O}_4$ ($x=0.12, 0.16, 0.20, 0.24, 0.28$) 尖晶石铁氧体, 研究 Cu 离子掺杂对其结构和介电性质的影响。XRD 结果表明所有样品均生成了单一的立方尖晶石结构, 并且晶格常数随着 Cu 掺杂量的增加而增加。通过扫描电镜观察到位于晶界处的白色颗粒为富 Cu 相。介电常数随频率变化曲线显示出尖晶石铁氧体典型的介电行为。但介电损耗随频率变化曲线则表现异常, 所有的 Cu 掺杂 Ni-Zn 铁氧体样品在某一频率下都表现出损耗峰。由于单位体积内 $\text{Fe}^{2+}/\text{Fe}^{3+}$ 之间跃迁的电子数目减少, $x=0.2$ 的样品电阻率最大, 而介电常数和介电损耗则最小。

关键词: 铁氧体; 铜离子掺杂; 介电常数; 介电色散; 介电损耗; 电阻率

(Edited by Yun-bin HE)